arXiv:1401.6021v2 [cond-mat.stat-mech] 28 Mar 2014

Pros and cons of swimming in a noisy environment

Piero Olla
ISAC-CNR and INFN, Sez. Cagliari, I–09042 Monserrato, Italy.
(Dated: February 28, 2024)

The problem of optimal microscopic swimming in a noisy environment is analyzed. A simplified model in which propulsion is generated by the relative motion of three spheres connected by immaterial links has been considered. We show that an optimized noisy microswimmer requires less power for propulsion (on average) than an optimal noiseless counterpart, migrating with identical mean velocity and swimming stroke amplitude. We also show that noise can be used to overcome some of the limitations of the scallop theorem, and have a swimmer that is able to propel itself with control over just one degree of freedom.

PACS numbers: 02.50.Ey,05.70.Ln,07.10.Cm,47.15.G-

I. INTRODUCTION

Microorganisms, such as bacteria and protozoa, live in a world governed by low-Reynolds number hydrodynamics. The strategies for locomotion in such an environment strongly differ from those valid at macroscopic scales [1]. This is exemplified by the content of the so called scallop theorem: a sequence of deformations in the body of a microswimmer will lead to the same displacement, irrespective of the speed at which each deformation is carried on. A "microscopic scallop" could not propel itself by quickly closing its valves, and then slowly opening them up to recover its initial configuration [2]. In order for propulsion to be achieved, the microswimmer must carry on a deformation sequence that does not trace itself back in time [3].

Progress in the field of nanotechnology has opened the way to the possible realization of artificial microswimmers [4–7]. One of the issues that will have to be solved is clearly that of the energy supply. This entails the optimization problem of finding the minimum energy strategy to propel the swimmer at the given velocity. Over the years, much attention has been given to this problem [8, 9]. Most of the effort has been directed to the study of "deterministic" microswimmers [9–13]. If the microswimmer is sufficiently small, however, thermal fluctuations will start to play a role, and the optimization problem will turn from deterministic to stochastic [14–18].

This aspect is of relevance to the new field of nanometer-scale swimming, in which propulsion is achieved by chemical unbalance in the environment, or on the surface of the nanodevice [19–21]. On the other hand, noise is expected to play a role also at larger scales, as the molecular motors responsible for propulsion, in a microswimmer, work in and out of equilibrium condition, and are likely to be characterized by fluctuations of larger amplitude than in thermal equilibrium [22].

The presence of noise will affect the swimmer performance in several ways. Noise will induce a random component in the swimming strokes, and therefore, also in the migration velocity [16, 18]. To this, global diffusion induced by thermal noise in the fluid, must be added. An optimal design is likely to require some minimization of these effects. At the same time, noise is likely to contribute to the energetics of the process. Here, things become less clear: it is well known that there are situations in which noise can play a constructive role. Most molecular motors, indeed, exploit thermal noise in some way or another to improve their efficiency [23].

This is precisely the question we want to ask: can thermal noise be exploited to improve the swimmer efficiency, and do part of the job of pushing the device along its desired path? The answer is yes, and we shall see that minimal dissipation, for given values of the mean swimming velocity, and of the swimming stroke amplitude, is achieved in correspondence to a minimum of the swimming velocity fluctuation. This does not correspond to a minimum of the random component in the swimming strokes, rather, it is realized through optimal control of their correlations. We shall discuss the nature of the internal forces in the swimmer that can produce this result.

To study the problem, we shall consider a swimmer design that has received much attention recently, namely, an ensemble of three

identical spherical beads connected by extendable links that do not interact with the fluid [12**?**]. Models in this class have been utilized to elucidate the properties both of individual swimmers [25, 26] and ensemble of swimmers [27, 28], and have found experimental realization, with optical tweezers used to drive the beads [7].

In order to proceed, we shall make a number of simplifying assumption on the structure of the swimmer, on the stroke amplitude and on the nature of the fluctuations. We shall assume that the swimmer moving parts and the stroke amplitude are small on the scale of the swimmer body, and that the dynamics of the system is slow. The first two assumptions allow a quasi-linear description of the dynamics, in which the feedback of the fluid perturbation on the swimmer dynamics, is disregarded. This corresponds to the lowest order in the description based on the Kirkwood-Smoluchowski equation, utilized in [18, 29]. The last assumption of slow dynamics guarantees that the response of the system to the deformation forces obey standard steady-state fluctuation-dissipation relations.

The paper is organized as follows. In Sec. 2, the main results on the optimization of the deterministic three-bead swimmer are presented. In Sec. 3, the modification of the problem in the presence of a noisy component in the swimmer internal dynamics are discussed. In Sec. 4, the optimization of the noisy swimmer in the weak noise limit is carried on. In Sec. 5, an example is provided, of how noise can be exploited to simplify the problem of internal control, by overcoming some of the limitation of the scallop theorem. Section 6 is devoted to conclusions.

II. DETERMINISTIC CASE

The microswimmer design that we are going to consider is a variation on the three-sphere model of Najafi & Golestanian [12, 30]. In the original swimmer the three spheres were put on the line, in the present one, they lie (at rest) at the vertices of an equilateral triangle. A similar model was used in [25, 31] to study passive swimming in an external flow. As in [12], the beads are supposed identical. We imagine that the device (called a trimer) is constrained to remain with its axis of symmetry along x_1, (see Fig. 1), but that it is otherwise free to translate. Consistent with this hypothesis, we

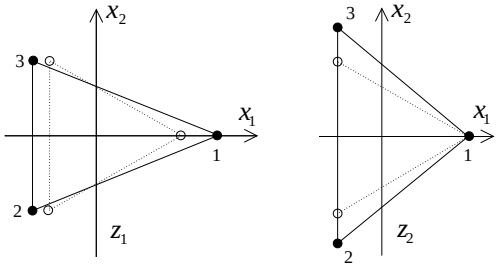


FIG. 1: Trimer deformations corresponding to $(z_1 > 0, z_2 = 0)$ (left) and $(z_1 = 0, z_2 > 0)$ (right). Empty circles indicate the rest shape.

assume that the trimer can undergo only axisymmetric deformations, as illustrated in Fig. 1. Let us indicate by $\mathbf{x}_i$, $i = 1, 2, 3$, the bead coordinates in the comoving frame, and separate the rest component $\mathbf{x}_i^{(0)}$:

$$\begin{aligned} \mathbf{x}_1^{(0)} &= R(1/\sqrt{3}, 0, 0), \\ \mathbf{x}_2^{(0)} &= R(-1/(2\sqrt{3}), -1/2, 0), \\ \mathbf{x}_3^{(0)} &= R(-1/(2\sqrt{3}), 1/2, 0), \end{aligned} \tag{1}$$

from the deformation component $\mathbf{x}_i^{(1)} = \mathbf{x}_i - \mathbf{x}_i^{(0)}$:

$$\begin{aligned} \mathbf{x}_1^{(1)} &= R(z_1/2, 0, 0), \\ \mathbf{x}_2^{(1)} &= (R/4)(-z_1, -\sqrt{3}z_2, 0), \\ \mathbf{x}_3^{(1)} &= (R/4)(-z_1, \sqrt{3}z_2, 0). \end{aligned} \tag{2}$$

The parametrization for $\mathbf{x}_i^{(1)}$ has been chosen in such a way that dissipation is diagonal [see Eq. (13) below)]. We shall assume small deformations:

$$R^{-1}|\mathbf{x}_i^{(1)}| \sim z \ll 1$$

and seek an expression for the migration velocity of the trimer to lowest order in z.

In creeping flow conditions, forces and particle velocities are related through the equation

$$\dot{\mathbf{x}}_i = \tilde{\mathbf{u}}_i(t) + \mathbf{f}_i(t)/\Gamma, \tag{3}$$

where Γ is the Stokes drag coefficient for the beads and $\tilde{u}_i$ is the flow perturbation generated by movement of the trimer, calculated at $\mathbf{x}_i$ (the fluid is considered quiescent in the absence of the trimer). For spherical beads, the drag Γ can be expressed in terms of the solvent kinematic viscosity ν_s and density ρ_s by means of the formula $\Gamma = 6\pi a \nu_s \rho_s$ [32]. The flow perturbation is determined by the instantaneous

velocity of the spheres through solution of the Stokes equations.

We assume that the spheres are small compared with the size of the trimer. This is basically a smallness assumption on the $\tilde{\mathbf{u}}_i(t)$ in Eq. (3), that scales indeed with a/R, with a the size of the beads. This allows the forces and the particle velocities to be connected by the linear relation (summation over repeated indices understood):

$$\tilde{\mathbf{u}}_i(t) = \mathbf{T}_{ij}\mathbf{f}_j; \quad \mathbf{T}_{ij} \equiv \mathbf{T}(\mathbf{x}_i - \mathbf{x}_j) \tag{4}$$

$$\mathbf{T}(\mathbf{x}) = \frac{3a}{4\Gamma}\Big[\frac{\mathbf{1}}{|\mathbf{x}|} + \frac{\mathbf{xx}}{|\mathbf{x}|^3}\Big], \tag{5}$$

where $\mathbf{T}$ is called the Oseen tensor [32]. Notice that, although we are assuming planar deformations, the equations leading to Eqs. (4-5) are those of 3D hydrodynamics.

We define a swimming cycle as a closed trajectory in deformation space: $\mathbf{z}(t + n\mathcal{T}) = \mathbf{z}(t)$ $\forall n$, that results in a finite displacement of the device center of mass $\mathbf{x}^{\rm CM} = \frac{1}{3}(\mathbf{x}_1 + \mathbf{x}_2 + \mathbf{x}_3)$: $\Delta\mathbf{x}^{\rm CM} = \mathbf{x}^{\rm CM}(t + \mathcal{T}) - \mathbf{x}^{\rm CM}(t) \neq 0$. The migration velocity is defined naturally as $\mathbf{u}^{migr} = \Delta\mathbf{x}^{\rm CM}/\mathcal{T}$. In the absence of external forces, $\sum_i \mathbf{f}_i = 0$, we find, from Eq. (3):

$$\mathbf{u}^{migr} = (1/3)\sum_i \langle\tilde{\mathbf{u}}_i\rangle_{\mathcal{T}} = \langle\tilde{\mathbf{u}}_1\rangle_{\mathcal{T}}, \tag{6}$$

where $\langle . \rangle_{\mathcal{T}}$ indicates time average over the stroke time $\mathcal{T}$.

The deformation sequence responsible for migration, in the case of the trimer, is illustrated in Fig. 2. The flow perturbations $\tilde{\mathbf{u}}_i$ in Eq. (6) are expressed in terms of the forces $\mathbf{f}_i$ by means of the Oseen tensor, Eqs. (4) and (5). These in turn can be expressed back in terms of the deformations, working to lowest order in a/R:

$$\mathbf{f}_i = \Gamma\dot{\mathbf{x}}_i = \Gamma\frac{\mathrm{d}\mathbf{x}_i(z_1, z_2)}{\mathrm{d}t} = \mathbf{s}_{ij}\dot{z}_j, \tag{7}$$

where the constant matrix $\mathbf{s}_{ij}$ is obtained from Eq. (2). From Eq. (4), we obtain the expression, valid to $O(a/R)$:

$$\mathbf{u}^{migr} = \frac{1}{3\mathcal{T}}\sum_i \oint_\gamma \mathbf{T}_{ij}\mathbf{s}_{jk}\mathrm{d}z_k \tag{8}$$

where γ indicates the closed path in z-space.

Equation (8) illustrates that migration cannot be achieved with a sequence of deformations that traces back in time. In particular, this implies that at least two degrees of freedom are necessary for microscopic swimming (scallop theorem [2, 3]). In order for the integral along γ to give non-zero result, it is necessary that the integrand is not an exact differential. We can Taylor expand the Oseen tensor in $\mathbf{z}$:

$$\mathbf{T}_{ij} = \mathbf{T}^{(0)}_{ij} + \mathbf{T}^{(1)}_{ijk}z_k + \dots$$

and we see that in order to obtain a non-zero migration velocity, we must keep terms up to $O(z)$ in the expansion for $\mathbf{T}$:

$$u^{migr} = \oint A_j \mathrm{d}z_j \equiv \Phi_{ij}\oint_\gamma z_i \mathrm{d}z_j$$

$$\Phi_{ij} = \frac{1}{3\mathcal{T}}\sum_l (\mathbf{T}^{(1)}_{lmi}\mathbf{s}_{mj})_1. \tag{9}$$

From here, simple algebra gives us (see Appendix A):

$$u^{migr} = -\frac{3\sqrt{3}a}{16\mathcal{T}}\int_0^{\mathcal{T}} [z_1\dot{z}_2 - z_2\dot{z}_1]\mathrm{d}t. \tag{10}$$

As discussed in [3, 13], the expression u^{migr} can be interpreted as the flux of the magnetic field

$$B = \epsilon_{3jk}\partial_{z_j}A_k = -\frac{3\sqrt{3}a}{8} \tag{11}$$

across the surface S in z-space, having γ for boundary. Thus, the swimming velocity is

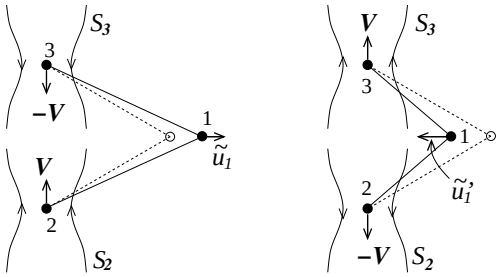


FIG. 2: Swimming strategy of the microswimmer. The length of 23 is varied periodically, $\pi/2$ out of phase with the the two lengths of 12 and 13. In this way, when the contraction (extension) speed of 23 is maximum, the horizontal extension of the triangle is minimum (maximum). Field lines $S_{2,3}$ describe the resulting perturbation in the fluid velocity. The asymmetry between the $\tilde{u}_1$ component experienced in the two cases causes migration in the negative x_1 direction.

purely controlled by the area S and by the time $\mathcal{T}$ necessary to go through the cycle.

The work that the trimer must execute to carry out a complete swimming cycle, coincides with the heat dissipated

$$Q = \int_0^{\mathcal{T}} \mathbf{f}_i(\tau) \cdot \dot{\mathbf{x}}_i(\tau) \mathrm{d}\tau, \tag{12}$$

which, from Eqs. (2) and (7), can be rewritten in terms of the deformation

$$Q = \frac{3\Gamma R^2}{8} \int_0^{\mathcal{T}} [(\dot{z}_1)^2 + (\dot{z}_2)^2] \mathrm{d}\tau. \tag{13}$$

We note at once, by comparison of Eqs. (10) and (13), that the migration velocity and the heat produced in one cycle scale, together with respect to z and $\mathcal{T}$: $Q \sim u^{migr} \sim z^2/\mathcal{T}$, and we have for the dissipated power $\dot{Q} \sim Q/\mathcal{T}$:

$$\dot{Q} \sim (u^{migr})^2/z^2;$$

smaller strokes produce less efficient swimming. Thus, in principle, dissipation could be sent to zero at finite swimming velocity (forgetting that we are working in a perturbative regime for z), by sending the swimming stroke amplitude and the stroke time $\mathcal{T}$ to infinity; a situation resembling the adiabatic ratchet described in [33].

Once the stroke amplitude is fixed, it remains to optimize stroke geometry. From $u^{migr} \sim z^2/\mathcal{T}$, we see that minimizing expended power at fixed u^{migr} and fixed stroke amplitude, is equivalent to minimize the heat dissipated in a swimming stroke at fixed u^{migr}. Formally, we need to minimize the functional $\mathcal{A} = Q[\mathbf{z}] + qu^{migr}[\mathbf{z}]$, with respect to $\mathbf{z}$, with boundary conditions $\mathbf{z}(\mathcal{T}) = \mathbf{z}(0)$. The constant q is the Lagrange multiplier required to implement the condition on u^{migr}.

Using Eqs. (9) and (13), reabsorbing constants, and rescaling time in unit of $\mathcal{T}$, the functional $\mathcal{A}$ takes the explicit form

$$\mathcal{A} = \int_0^{\mathcal{T}} [|\dot{\mathbf{z}}|^2/2 + q\mathbf{A} \cdot \dot{\mathbf{z}}] \mathrm{d}t. \tag{14}$$

This is the action for a unit mass – charge q particle, moving in a uniform magnetic field $\mathbf{B} = \nabla_z \times \mathbf{A}$. The optimal strategy for the microswimmer corresponds to the trajectory in deformation space that solves the variational problem $\delta\mathcal{A} = 0$. We thus recover the result in [13] that the optimization of the microswimmer can be mapped to the problem of a charged particle in a uniform magnetic field. The fact that B can be approximated as uniform (which is consequence of the smallness of z), implies that any trajectory $\mathbf{z}(t)$, obtained from translation of an extremal trajectory for $\mathcal{A}$, will be extremal as well. The degeneracy can be removed imposing the condition that the undeformed state $\mathbf{z} = 0$ is really the rest shape for the swimmer. This can be expressed as a condition on the time average of the deformation:

$$\langle \mathbf{z} \rangle_{\mathcal{T}} = 0. \tag{15}$$

The end result is uniform circular motion in deformation space, with angular frequency qB and center in $\mathbf{z} = 0$:

$$\mathbf{z}(t) = \bar{z}_0 \Big(\cos(\alpha + qBt), \sin(\alpha + qBt) \Big). \tag{16}$$

We notice that this solution is characterized by constant dissipated power. The boundary condition $\mathbf{z}(t + \mathcal{T}) = \mathbf{z}(t)$ fixes the value of the Lagrange multiplier: $q = \pm 2\pi/(B\mathcal{T})$. Using Eq. (16) in Eqs. (13) and (10), we obtain the optimal values

$$\bar{Q} = \frac{3\pi^2 \Gamma R^2 \bar{z}_0^2}{2\mathcal{T}}, \quad \bar{u}^{migr} = \frac{3\sqrt{3}\pi a \bar{z}_0^2}{8\mathcal{T}}, \tag{17}$$

where we have taken $q < 0$ to have positive u^{migr}. Notice that $\bar{Q}$ and $\bar{u}^{migr}$ scale together with respect to z and $\mathcal{T}$, which is a consequence of Eqs. (10) and (13), i.e. of the small stroke amplitude assumption. This suggests us to adopt the definition of efficiency given in [34]:

$$\eta = u^{migr}/Q, \tag{18}$$

and η will be independent of z in the small stroke amplitude regime considered. Notice that, for fixed u^{migr} and $\mathcal{T}$, the definition becomes equivalent to the one in [8], that was basically $\eta' = (u^{migr})^2/\dot{Q}$. From Eq. (17), we obtain the optimal efficiency:

$$\bar{\eta} = \bar{u}^{migr}/\bar{Q} = \frac{\sqrt{3}}{4\pi} \frac{a}{\Gamma R^2}. \tag{19}$$

III. CASE WITH THERMAL NOISE

In the presence of noise, quantities entering the optimization procedure, such as Q and

u^{migr}, acquire a fluctuating component. This forces us to work with averages, rather than with instantaneous quantities. [For instance, Eq. (15) will now be understood in a statistical sense: $\langle \mathbf{z} \rangle = 0$. Likewise, the swimming efficiency Eq. (18) will generalize to $\eta = \langle u^{migr} \rangle / \langle Q \rangle$]. At the same time, the swimming stroke will no longer be associated with a closed orbit in deformation space, and the stroke time $\mathcal{T}$ must be interpreted as a characteristic deformation time of the device.

The choice of the statistical quantities to minimize, and of the constraints to impose in the optimization procedure, strongly rests on the specific problem in which one is interested. A swimmer that wants to hit a target in the shortest possible time, may have uncertainty (the variance of u^{migr}) among the quantities to minimize or to use as constraints. For the long time – steady state regime we are interested in, the most natural choice is that of minimizing expended power. We thus impose minimization of the mean expended power $\langle \dot{Q} \rangle$ at fixed mean migration velocity $\langle u^{migr} \rangle$. Supported by the observation that optimal noiseless swimming is achieved at constant $\dot{Q}$ [and at constant value of the rate $z_1 \dot{z}_2 - z_2 \dot{z}_1$ in Eq. (10)], we shall restrict our analysis to a stationary statistics condition.

We focus on a situation in which the internal forces vary slowly on the scale of the relaxation time of the system. This condition appeared to be crucial in stochastic optimization problems involving a finite time horizon [35], due to the occurrence of singularities in the solution [36]. In [37], the problem was avoided by regularization (see also [38, 39]). This is not an issue for the stationary regime considered here, and the main advantage of an overdamped regime, is that the dynamics is described by a simple Langevin equation, and that steady state fluctuation-dissipation relations do apply.

The relaxation time can be estimated, in the case of the trimer, by the Stokes time of the beads $\tau_S = m/\Gamma$, where m is the bead mass [32]. For spherical beads of radius a and density $\rho_b = \lambda \rho_s$: $\tau_S = (2/9)\lambda a^2/\nu_s$, with ν_s and ρ_s the kinematic viscosity and the density of the solvent. Under the condition $\tau_S \ll \mathcal{T}$, the dynamics will be described by a Langevin equation

$$\dot{\mathbf{z}} + \mathbf{g} = \boldsymbol{\xi}, \quad \langle \xi_i(t) \xi_j(0) \rangle = 2K \delta_{ij} \delta(t), \quad (20)$$

where, imposing validity of the equilibrium fluctuation-relations, and making use of Eq. (13):

$$K = \frac{8 k_B T}{3 \Gamma R^2}, \quad (21)$$

with k_B the Boltzmann constant and T the temperature [42]. The mean dissipation is obtained from generalization of Eq. (12):

$$\langle \dot{Q} \rangle = (3\Gamma R^2/8) \langle \dot{\mathbf{z}}(t) \circ \mathbf{g}(t) \rangle, \quad (22)$$

where the $\circ$ in the scalar product indicates Stratonovich prescription [40, 41]. Similarly for the mean migration velocity, that is obtained generalizing Eq. (10):

$$\langle u^{migr} \rangle = -\frac{3\sqrt{3}a}{16} \langle [z_1 \dot{z}_2 - z_2 \dot{z}_1] \rangle, \quad (23)$$

and it is easy to see, from Eq. (20), that the term in the average does not depend on the choice of the stochastic prescription.

The presence of noise induces a diffusive component in migration, which receives contribution both from thermal noise in the fluid and random swimming. The first contribution to diffusivity can be estimated as

$$D^{ext} \sim K R^2. \quad (24)$$

The second can be obtained from

$$D^{int} = \int \mathrm{d}t \langle \hat{u}(t) \hat{u}(0) \rangle,$$

where

$$\hat{u} = -\frac{3\sqrt{3}a}{16} [z_1 \dot{z}_2 - z_2 \dot{z}_1] - \langle u^{migr} \rangle$$

is the fluctuating component of the migration velocity. Working in polar coordinates (z, ϕ), we can write $z_1 \dot{z}_2 - z_2 \dot{z}_1 = z^2 \dot{\phi}$, and, using Eq. (20):

$$D^{int} = \frac{27 a^2}{256} \Big[2K + \int \mathrm{d}t \, \langle z(t) g_\phi(t) z(0) g_\phi(0) \rangle_c \Big]. \quad (25)$$

In the present situation, in which noise results from equilibrium fluctuations in the fluid, and the moving parts in the swimmer are small, global diffusion, Eq. (24), will dominate over random swimming, Eq. (25). In realistic situations, internal noise acquires a non-equilibrium

component [22], and one should make a substitution $K \to K^{int} \gg K$ in both Eqs. (20) and (25). (At that point, the possibility of a finite noise correlation time, should probably be taken into account). Furthermore, an optimal swimmer should have $a \sim R$ [see Eqs. (17) and (23)]. Thus, in realistic situations, random swimming is expected to dominate over global diffusion, $D^{int} \gg D^{ext}$, and it becomes meaningful to minimize D^{int} along with $\langle Q \rangle$.

IV. WEAK NOISE

For sufficiently weak noise, we expect that the swimming strategy of the optimal noisy swimmer, will be sufficiently close to the one in the noiseless case. With this, we intend that the orbits in deformation space will remain close to the circular orbit of the optimal noiseless swimmer. This imposes the condition on the noise amplitude

$$\tilde{K} = \frac{K}{\omega \bar{z}_0^2} \ll 1, \tag{26}$$

where $\omega \equiv 2\pi/\mathcal{T}$ is defined here as the mean circulation frequency in deformation space; in polar coordinates: $\langle \dot{\phi} \rangle = \omega$.

Working in polar coordinates, the equation of motion (20) will read:

$$\dot{z} = g_z + \frac{K}{z} + \xi_z, \quad \dot{\phi} = \frac{1}{z} g_\phi + \frac{1}{z} \xi_\phi,$$
$$\langle \xi_i(t) \xi_j(0) \rangle = 2K \delta_{ij} \delta(t). \tag{27}$$

In view of a small-noise expansion of Eq. (27), we introduce rescaled variables $s = (z - \bar{z}_0)/\bar{z}_0$, $\psi = \phi - \omega t$, $\tilde{t} = \omega t$, giving the deviation of the phase point of the noisy swimmer from its optimized noiseless counterpart (see Fig. 3). The forces are rescaled in consequence:

$$\tilde{g}_s = \frac{g_z}{\bar{z}_0 \omega}; \qquad \tilde{g}_\psi = -1 + \frac{g_\phi}{z\omega}. \tag{28}$$

Notice that, in rescaled variables, the definition $\langle \dot{\phi} \rangle = \omega$ translates in the constraint $\langle \dot{\psi} \rangle = 0$, i.e. $\langle \tilde{g}_\psi \rangle = 0$. Consistent with the assumption of small deviation from circular orbit, we impose linear dependence of the forces on s:

$$\tilde{g}_i = -\alpha_{is}(\psi, \tilde{t}) s + h_i(\psi, \tilde{t}), \quad i = s, \psi, \tag{29}$$

and assume $\alpha_{is} = O(1)$.

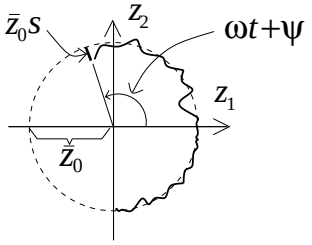


FIG. 3: Sketch of a $\tilde{K} \ll 1$ optimal trajectory in deformation space. The phase point is expected to depart little from the noiseless optimal orbit (the dashed circle). The coordinates ψ and $\bar{z}_0 s$ give the separation between the phase point of the noisy and the deterministic optimal trimer.

Substituting Eq. (28) into Eq. (27), and keeping terms up to $O(\tilde{K})$, we obtain the equation of motion

$$\dot{s} = \tilde{g}_s + \tilde{K} + \xi_s; \quad \dot{\psi} = \tilde{g}_\psi + \xi_\psi;$$
$$\langle \xi_i(0) \xi_j(\tilde{t}) \rangle = 2\tilde{K} \delta_{ij} \delta(\tilde{t}). \tag{30}$$

The migration velocity is obtained, substituting Eqs. (27) and (28) into Eq. (23):

$$\langle u^{migr} \rangle = \bar{u}^{migr} \langle (1+s)^2 [1 + \tilde{g}_\psi(s, \psi)] \rangle, \tag{31}$$

and we recover, for $\tilde{K} = 0$, Eq. (17). In analogy with Sec. 2, we choose to minimize $\langle \dot{Q} \rangle$ at fixed $\langle z \rangle = \bar{z}_0$ and $\langle u^{migr} \rangle$, that is equivalent, from Eqs. (17) and (31), to minimizing $\langle Q \rangle = \mathcal{T} \langle \dot{Q} \rangle$ at fixed $\langle u^{migr} \rangle$. Substituting Eqs. (27) and (28) into Eq. (22), we obtain:

$$\langle Q \rangle = \bar{Q} \Big\langle \Big[\tilde{g}_s^2 + [(1+s)(1+\tilde{g}_\psi)]^2 + \tilde{K} \nabla \cdot \tilde{\mathbf{g}} \Big] \Big\rangle, \tag{32}$$

where the term $\tilde{K} \nabla \cdot \tilde{\mathbf{g}}$ accounts for the correction from the Stratonovich prescription [41]. Again we recover, for $\tilde{K} = 0$, the expression for dissipation provided in Eq. (17).

To determine the difference between minimum dissipation with and without noise, we fix $\langle u^{migr} \rangle = -\bar{u}^{migr}$, and study the behavior of $\mathcal{A} = \langle Q \rangle / \bar{Q}$, under the combined constraints $\langle u^{migr} \rangle / \bar{u}^{migr} = 1$ and $\langle \tilde{g}_\psi \rangle = 0$. Notice that we can write also $\mathcal{A} = \bar{\eta}/\eta$, with $\eta = \langle u^{migr} \rangle / \langle Q \rangle$ and $\bar{\eta}$ the optimal efficiency of the deterministic swimmer, given by Eq. (19).

Using Eqs. (30) and (31), the two constraints give, including terms up to $O(\tilde{K})$:

$$\langle \tilde{g}_\psi \rangle = 0; \qquad 2\langle s \rangle + \langle s^2 \rangle + 2\langle s \tilde{g}_\psi \rangle = 0. \tag{33}$$

Substituting into Eq. (32) and keeping terms up to $O(\tilde{K})$, we finally get:

$$\begin{aligned}\mathcal{A} &= \Big\langle \Big\{ 1 + 2s\tilde{g}_\psi + \tilde{g}_s^2 + \tilde{g}_\psi^2 \\ &+ \tilde{K}(\partial_s \tilde{g}_s + \partial_\psi \tilde{g}_\psi) \Big\} \Big\rangle, \end{aligned} \tag{34}$$

where the 1 comes from dissipation in the deterministic case. We see that, contrary to the noiseless case of Eq. (14), the forces now enter explicitly the normalized dissipation $\mathcal{A}$. This reflects the fact that, while in the noiseless case one had a single optimal trajectory, in the presence of noise, we have a distribution of trajectories whose shape is determined by the force $\tilde{\mathbf{g}}$. If we restrict the analysis to the case of a stationary swimmer, the coefficients α_{is} and h_i will be independent of time as well. We shall consider below two specific driving mechanisms:

- A uniform tangential force pushing the phase point, while some constant radial force keeps it close to the unperturbed orbit $z = \bar{z}_0$.

- A potential well confining the phase points both tangentially and radially. The potential well circulates along the optimal noiseless orbit $r = \bar{z}_0$ with angular frequency ω.

In the first case, the stationary distribution of the phase points will be localized in a uniform thickness annulus around the optimal noiseless orbit $z = \bar{z}_0$. In the second case, the stationary distribution will be localized both in z and in ϕ, and will circulate with frequency ω along the orbit $z = \bar{z}_0$.

In a realistic swimmer, the driving mechanism may be provided e.g. by a molecular motor undergoing some cyclic transformation. The two driving mechanisms outlined above, may correspond therefore to the two regimes of a fluctuating and a fluctuation-free motor respectively. In the first case, the fluctuations in the motor configuration would sum to those in the interaction with the swimmer moving parts, causing global diffusion of $\mathbf{z}$ along the deterministic orbit. In the second case, the only fluctuation present would be those in the interaction between molecular motor and swimmer moving parts, while the molecular motor dynamics is deterministic.

A. Uniform tangential drive

In this case, the coefficients α_{is} and h_i in Eq. (29) are independent of ψ. The linear Langevin equations (30) are presently solved. At stationary state, the phase points are localized radially,

$$\langle s^2 \rangle = \frac{\tilde{K}}{\alpha_{ss}}, \quad \langle s \rangle = \frac{h_s + \tilde{K}}{\alpha_{ss}}, \tag{35}$$

and uniformly distributed in ψ. Imposing the conditions (33), we find from Eqs. (29) and (30):

$$\begin{aligned} h_s &= (\alpha_{\psi s} - 3)\tilde{K}/2, \\ h_\psi &= (\alpha_{\psi s} - 1)\alpha_{\psi s}\tilde{K}/(2\alpha_{ss}), \end{aligned} \tag{36}$$

and α_{is}, $i = s, \psi$, remain the only free parameters. Substituting Eqs. (35) and (36), together with Eq. (29), into Eq. (34), and keeping terms up to $O(\tilde{K})$, we obtain

$$\mathcal{A} = 1 + \frac{\tilde{K}\alpha_{\psi s}}{\alpha_{ss}}(\alpha_{\psi s} - 2). \tag{37}$$

For $0 < \alpha_{\psi s} < 2$, dissipation is reduced with respect to the noiseless case, the effect being maximum at $\alpha_{\psi s} = 1$. In this range, efficiency is increased with respect to the optimal noiseless case of Eq. (19): $\eta > \bar{\eta}$. Dissipation reduction is associated with decrease of the tangential drive for larger deformations.

B. Circulating potential well

In this case, the phase points are confined both radially and tangentially, in a potential well that rotates uniformly with frequency ω. If the confinement length is small also tangentially, we can linearize the forces also with respect to ψ:

$$\begin{aligned} \tilde{g}_s &= -\alpha_{ss}(s - \bar{s}_s) - \alpha_{s\psi}\psi, \\ \tilde{g}_\psi &= -\alpha_{\psi s}(s - \bar{s}_\psi) - \alpha_{\psi\psi}\psi, \end{aligned} \tag{38}$$

where again we assume $\alpha_{ij} = O(1)$. The equations of motion are still those in Eq. (30), and the constraints in Eq. (33) continue to apply. As in the case of the coefficients h_i of Eq. (36), it is possible to see that $\bar{s}_i = O(\tilde{K})$, and therefore also $\langle s \rangle = \langle \psi \rangle = O(\tilde{K})$. Substituting Eq.

(38) into Eq. (34), we obtain, keeping terms up to $O(\tilde{K})$:

$$\begin{aligned}\mathcal{A} &= 1+(\alpha_{ss}^2+\alpha_{\psi s}^2-2\alpha_{\psi s})\langle s^2\rangle \\ &+ (\alpha_{\psi\psi}^2+\alpha_{s\psi}^2)\langle\psi^2\rangle \\ &+ 2[\alpha_{ss}\alpha_{s\psi}+(\alpha_{\psi s}-1)\alpha_{\psi\psi}]\langle s\psi\rangle \\ &- (\alpha_{ss}+\alpha_{\psi\psi})\tilde{K}. \end{aligned} \quad (39)$$

The equation for the correlations entering Eq. (39) are obtained from Eqs. (30) and (38). At stationary state:

$$\begin{aligned}&\alpha_{ss}\langle s^2\rangle+\alpha_{s\psi}\langle s\psi\rangle=\tilde{K},\\ &\alpha_{\psi s}\langle s^2\rangle+(\alpha_{ss}+\alpha_{\psi\psi})\langle s\psi\rangle+\alpha_{s\psi}\langle\psi^2\rangle=0,\\ &\alpha_{\psi s}\langle s\psi\rangle+\alpha_{\psi\psi}\langle\psi^2\rangle=\tilde{K}. \end{aligned} \quad (40)$$

The solutions of Eq. (40) have in general a rather complicated form. We can solve the system explicitly in some special situation.

In the case of a purely potential $\tilde{\mathbf{g}}$, which implies $\alpha_{s\psi}=\alpha_{\psi s}$, Eq. (40) gives

$$\begin{aligned}\langle s^2\rangle &= \frac{\alpha_{\psi\psi}\tilde{K}}{\alpha_{ss}\alpha_{\psi\psi}-\alpha_{s\psi}^2};\\ \langle s\psi\rangle &= \frac{-\alpha_{s\psi}\tilde{K}}{\alpha_{ss}\alpha_{\psi\psi}-\alpha_{s\psi}^2};\\ \langle\psi^2\rangle &= \frac{\alpha_{ss}\tilde{K}}{\alpha_{ss}\alpha_{\psi\psi}-\alpha_{s\psi}^2}.\end{aligned}$$

Substituting into Eq. (39), it is possible to see that $\mathcal{A}=1$, which is the expected result from a purely potential force.

Things change if we consider a dissipative force. Let us take for simplicity $\alpha_{ss}=\alpha_{\psi\psi}$ and $\alpha_{\psi s}=-\alpha_{s\psi}$. We obtain

$$\langle s^2\rangle=\langle\psi^2\rangle=\tilde{K}/\alpha_{ss}, \qquad \langle s\psi\rangle=0,$$

which, upon substitution into Eq. (39) gives

$$\mathcal{A}=1+2\frac{\alpha_{\psi s}\tilde{K}}{\alpha_{ss}}(\alpha_{\psi s}-1). \quad (41)$$

Dissipation reduction occurs in this case for $0<\alpha_{\psi s}<1$, corresponding to an increase of efficiency with respect to the optimal noiseless case $\eta>\bar{\eta}$. Maximum reduction occurs at $\alpha_{\psi s}=1/2$ [compare with Eq. (37)].

C. Randomness minimization

An optimal microswimmer should have the property of "arriving at the target on time", if required. Thus, another quantity that one may wish to minimize is the migration velocity fluctuation. For simplicity, we keep considering the situation of a stationary swimmer, although the appropriate setting for such a constraint is that of a device swimming over a finite distance (or over a finite time interval).

One way to minimize swimming randomness, of course, is to make the deterministic part of the forces, controlling the trimer deformation, more intense. For fixed strength of the deformation forces, some swimming strategies will nevertheless lead to a smaller migration velocity fluctuation than others. We see that in both cases of forcing by a uniform drive, and by a circulating potential well, minimization of the random migration velocity component is achieved, in good approximation, together with that of dissipation.

We parametrize the degree of randomness in swimming through the coefficient $\tilde{D}=(\omega/(\bar{u}^{migr})^2)D^{int}$, where D^{int} is defined in Eq. (25). Substituting Eq. (28) into Eq. (25), we obtain, keeping terms up to $O(\tilde{K})$:

$$\begin{aligned}\tilde{D} &= 2\tilde{K}+\int \mathrm{d}\tilde{t}\,\Big[4\langle s(0)s(\tilde{t})\rangle \\ &+ 4\langle s(0)\tilde{g}(\tilde{t})\rangle+\langle\tilde{g}_\psi(0)\tilde{g}_\psi(\tilde{t})\rangle\Big]. \end{aligned} \quad (42)$$

In the uniform tangential drive case, we have $\tilde{g}_\psi=-\alpha_{\psi s}+O(\tilde{K})$. From Eqs. (28) and (30), we find $\langle s(0)s(\tilde{t})\rangle=(\tilde{K}/\alpha_{ss})\exp(-\alpha_{ss}|\tilde{t}|)$, and, substituting into Eq. (42):

$$\tilde{D}=\frac{2\tilde{K}}{\alpha_{ss}^2}\Big(4+\alpha_{ss}^2+2\alpha_{\psi s}(\alpha_{\psi s}-2)\Big). \quad (43)$$

Comparing with Eq. (37), we see that minimal contribution to diffusion from random swimming is achieved, together with minimal dissipation, for $\alpha_{\psi s}=1$.

In the case of a forcing by a circulating potential well, with $\alpha_{\psi\psi}=\alpha_{ss}$ and $\alpha_{s\psi}=\alpha_{\psi s}$, we proceed in the same fashion. We have, to lowest order in $\tilde{K}$: $\tilde{g}_s=-\alpha_{ss}s-\alpha_{\psi\psi}\psi$ and $\tilde{g}_\psi=-\alpha_{ss}\psi+\alpha_{\psi\psi}s$, which gives, from Eqs. (28) and (30): $\langle s(0)s(\tilde{t})\rangle=\langle\psi(0)\psi(\tilde{t})\rangle=(\tilde{K}/\alpha_{ss})\exp(-\alpha_{ss}|\tilde{t}|)$ and $\langle s(0)\psi(\tilde{t})\rangle=0$. Substituting into Eq. (42), we find

$$\tilde{D}=\frac{2\tilde{K}}{\alpha_{ss}^2}\Big(4+\alpha_{ss}^2+\alpha_{\psi s}(\alpha_{\psi s}-4)\Big). \quad (44)$$

Comparing with Eq. (41), we find that dissipation reduction implies random swimming re-

duction, but not vice versa. In this case, minimum random swimming occurs for $\alpha_{\psi s} = 2$, that is out of the domain in which there is dissipation reduction.

V. STRONG NOISE

We consider now the situation in which the random component of the deformations cannot be considered as a perturbation. In [31], it was suggested that noise could be used to circumvent some of the limitations of the scallop theorem, namely the need of control over at least two degrees of freedom to achieve locomotion. We are going to provide an example of this effect, assuming that the only degree of freedom acted upon in the trimer by a driving force, is the transversal one z_2 (see Fig. 1), while the longitudinal one z_1 is bound by a constant elastic force.

We put in Eq. (20), $g_1 = -\omega z_1$ and $g_2 = \omega\tilde{g}(\mathbf{z})$, where ω fixes the deformation time scale of the problem, and $\tilde{g}(\mathbf{z})$ contains the drive. The equations of motion thus become, rescaling time $t \to \tilde{t} = \omega t$:

$$\begin{aligned} &\dot{z}_1 + z_1 = \xi_1; \quad \dot{z}_2 - \tilde{g}(\mathbf{z}) = \xi_2 \\ &\langle \xi_i(0)\xi_j(\tilde{t})\rangle = 2\tilde{K}\delta_{ij}\delta(\tilde{t}), \end{aligned} \tag{45}$$

where now $\tilde{K} = K/\omega$. Proceeding from Eqs. (22) and (23), we find for the mean expended power

$$\langle \dot{Q}\rangle = \frac{3\Gamma\omega^2 R^2}{8}\langle[\tilde{g}^2 + \tilde{K}\partial_{z_2}\tilde{g}]\rangle, \tag{46}$$

where the $\tilde{K}\partial_{z_2}\tilde{g}$ is the correction from the Stratonovich prescription [41]. Similarly for the mean migration velocity:

$$\langle u^{migr}\rangle = -\frac{3\sqrt{3}a\omega}{16}\langle[z_1(z_2+\tilde{g})]\rangle. \tag{47}$$

We determine the form of the drive $\tilde{g}$, minimizing $\langle\dot{Q}\rangle$ at fixed $\langle u^{migr}\rangle$. The stationary Fokker-Planck equation associated with Eq. (45) will be

$$\mathcal{L}^+\rho = \partial_{z_1}(z_1\rho) - \partial_{z_2}(\tilde{g}\rho) + \tilde{K}\nabla^2_{\mathbf{z}}\rho = 0, \tag{48}$$

where $\rho = \rho(\mathbf{z})$ is the stationary probability density function for $\mathbf{z}$. As we do not know in advance the form of $\rho(\mathbf{z})$, we must minimize heat production under the two constraints that $\langle u^{migr}\rangle$ is given, and that ρ obeys Eq. (48). We cannot disregard this last constraint, as the averages in Eqs. (46) and (47) are carried out precisely with $\rho(\mathbf{z})$. Our cost function will be therefore in the form

$$\begin{aligned} \mathcal{A} &= \langle\dot{Q}\rangle - q\langle u^{migr}\rangle \\ &+ \int \mathrm{d}z_1\mathrm{d}z_2\ J(\mathbf{z})\mathcal{L}^+\rho(\mathbf{z}), \end{aligned}$$

with $J(\mathbf{z})$ the new Lagrange multiplier, required to guarantee satisfaction locally of Eq. (48). Reabsorbing constants in $\mathcal{A}$, q and J, and integrating by parts where necessary, we obtain

$$\begin{aligned} \mathcal{A} &= \int \mathrm{d}z_1\mathrm{d}z_2\ \rho\Big\{\tilde{g}^2 - \tilde{K}\tilde{g}\partial_{z_2}\ln\rho \\ &+ qz_1(z_2+\tilde{g}) \\ &+ \Big[\tilde{K}\nabla^2_{\mathbf{z}} - z_1\partial_{z_1} + \tilde{g}\partial_{z_2}\Big]J\Big\}. \end{aligned} \tag{49}$$

Our optimal g is obtained taking the variation of $\mathcal{A}$ with respect to g and ρ, and equating to zero:

$$\begin{aligned} \frac{\delta\mathcal{A}}{\delta\tilde{g}} &= \rho\Big[-2\tilde{g} + \tilde{K}\partial_{z_2}\ln\rho - qz_1 - \partial_{z_2}J\Big] = 0; \\ \frac{\delta\mathcal{A}}{\delta\rho} &= \tilde{g}^2 + \tilde{K}\partial_{z_2}\tilde{g} + qz_1(z_2+\tilde{g}) \\ &+ \Big[\tilde{K}\nabla^2_{\mathbf{z}} - z_1\partial_{z_1} + \tilde{g}\partial_{z_2}\Big]J = 0. \end{aligned} \tag{50}$$

We see that Eq. (50) has solution in the form $\tilde{g} = -\alpha z_1 - \beta z_2$, with quadratic $\ln\rho$ and J. The optimal dynamics is thus linear:

$$\dot{z}_1 + z_1 = \xi_1; \quad \dot{z}_2 + \alpha z_1 + \beta z_2 = \xi_2. \tag{51}$$

The correlation equations associated with Eq. (51) are $\langle z_1^2\rangle = \tilde{K}$; $(1+\beta)\langle z_1 z_2\rangle + \alpha\langle z_1^2\rangle = 0$ and $\alpha\langle z_1 z_2\rangle + \beta\langle z_2^2\rangle = \tilde{K}$, that give us:

$$\begin{aligned} &\langle z_1^2\rangle = \tilde{K}; \quad \langle z_1 z_2\rangle = -\frac{\alpha\tilde{K}}{1+\beta}; \\ &\langle z_2^2\rangle = \frac{\alpha^2+\beta+1}{\beta(1+\beta)}\tilde{K}. \end{aligned} \tag{52}$$

Substituting into Eqs. (46) and (47), we obtain

$$\langle\dot{Q}\rangle = \frac{3\Gamma\omega^2R^2}{8}\frac{\alpha^2\tilde{K}}{1+\beta}, \tag{53}$$

and

$$\langle u^{migr}\rangle = -\frac{3\sqrt{3}\omega a}{8}\frac{\alpha\tilde{K}}{1+\beta}. \tag{54}$$

so that $\langle \dot{Q} \rangle \sim \alpha\omega \langle u^{migr} \rangle$.

From Eq. (51), it appears that $\alpha\omega$ plays the role of circulation frequency for the trimer. Its inverse fixes the scale for the stroke time $\mathcal{T}$. We see that, as in the deterministic case, expended power can be made smaller by increasing $\mathcal{T}$. For fixed $\langle u^{migr} \rangle$, this will correspond to larger swimming strokes. From Eq. (54), $\langle u^{migr} \rangle$ fixes in fact $\alpha/(1+\beta)$, so that smaller α will require smaller β. This in turn corresponds to larger swimming strokes [see Eq. (52)]. Similarly, making ω small, will lead to larger $\tilde{K}$, and therefore to larger swimming strokes [see again Eq. (52)].

The efficiency of the swimmer $\eta = \langle u^{migr} \rangle / \langle Q \rangle$ can be determined from Eqs. (53) and (54), once the stroke time $\mathcal{T}$ is known: $\langle Q \rangle = \mathcal{T} \langle \dot{Q} \rangle$. Unfortunately, contrary to the weak noise case, the circulation frequency distribution in deformation space is not peaked around a well-defined value that could uniquely define the stroke frequency. (Similarly for the stroke amplitude z, that is not peaked around the deterministic value $\bar{z}_0$). We can nevertheless define a stroke time in terms of the mean circulation frequency: $\omega\mathcal{T} = 2\pi/\langle \dot{\phi} \rangle$, $\phi = \tan^{-1} z_2/z_1$, and compare with the optimal deterministic case. A calculation, detailed in Appendix B, shows that the efficiency of a swimmer whose internal dynamics is governed by a linear Langevin equation, such as Eq. (51), is always smaller than that of an optimal deterministic swimmer with identical $\mathcal{T}$. This seems to confirm the result in the weak noise regime, that dissipation reduction must involve some kind of drive reduction at large deformations. This is in fact the opposite of the situation described in Eq. (51) (or in any dynamics described by a Langevin dynamics with center at $\mathbf{z} = 0$).

VI. CONCLUSION

We have discussed the possibility of dissipation reduction by thermal noise in a simple microswimmer model. We have shown that an optimal noisy microswimmer will need, for propulsion at given average swimming velocity and swimming stroke amplitude, less energy than its noiseless optimal counterpart, and that the process goes together with reduction in randomness of the swimming velocity. Another effect of noise is that some of the constraints of the scallop theorem can be bypassed, as the swimmer can propel itself with control over just one degree of freedom.

The optimal design of a noisy microswimmer, imposes constraints on the functional form of the deformation forces driving its dynamics, that are not present in the deterministic case [13]. The need to optimize a distribution of deformation sequences, rather than a single deformation sequence stands at the basis of the new constraints. We have determined the optimal deformation force profiles in both strong and weak noise conditions.

We stress that the results obtained are valid only for a regime of small moving parts and small swimming strokes. A detailed numerical analysis would be required to confirm our results, in the case of an optimal microswimmer with moving parts and swimming strokes comparable in size with the swimmer body.

Another issue that should probably be addressed is the robustness of the results, with respect to modification in the form of the noise [e.g. as regards possible finiteness of the correlation time in Eq. (20)].

Throughout this paper, we have considered the case of a stationary swimmer, which is consistent with focus on average quantities such as the mean expended power $\langle \dot{Q} \rangle$ and the mean migration velocity $\langle u^{migr} \rangle$. In a general finite time horizon situation, the statistics will be time dependent, and other quantities beyond $\langle \dot{Q} \rangle$ and $\langle u^{migr} \rangle$ are expected to play a role in the optimization process.

We must remember that, even in the case of an infinite time horizon, stationarity is an assumption. We have not examined e.g. the case of a swimmer for which $\langle \dot{Q} \rangle$ and $\langle u^{migr} \rangle$ have a component that is periodic in time. Minimization in this case would be still performed working with the constant components of $\langle \dot{Q} \rangle$ and $\langle u^{migr} \rangle$, but the space of possible swimming strategies is larger than in the constant case. Thus, we do not rule out the possibility that swimming strategies admitting periodic components in $\langle \dot{Q} \rangle$ and $\langle u^{migr} \rangle$ may have better properties than the ones considered in the present analysis.

Appendix A: Determination of the migration velocity in the deterministic case

The migration velocity in the deterministic case is obtained substituting Eqs. (3) and (4) into Eq. (6). Exploiting equality of the contribution to $\tilde{\mathbf{u}}_1$ from particles 2 and 3, we can write:

$$u^{migr} \simeq 2\Gamma\langle[T^{(1)}_{12,11}\dot{x}^{(1)}_{2,1} + T^{(1)}_{12,12}\dot{x}^{(1)}_{2,2}]\rangle_{\mathcal{T}}, \quad \text{(A1)}$$

and we adopt the convention that, in vector and tensor expressions, indices before comma indicate particle labels; after comma, they indicate vector components.

A little algebra from Eqs. (1-2) and (4-5) gives us

$$\begin{aligned} T_{12,11} &= \sigma\Big(\frac{7}{4} - \frac{\sqrt{3}}{32}(9z_1 - 5z_2)\Big), \\ T_{12,12} &= \sigma\Big(\frac{3\sqrt{3}}{16} - \frac{9}{32}(3z_1 + z_2)\Big), \quad \text{(A2)} \end{aligned}$$

where $\sigma = 3a/(4\Gamma R)$. Substituting Eq. (A2) into Eq. (A1), we obtain

$$\begin{aligned} u^{migr} &\simeq \frac{3\sqrt{3}a}{265}\langle 5z_2\dot{z}_1 - 27z_1\dot{z}_2\rangle_{\mathcal{T}} \\ &= -\frac{3\sqrt{3}a}{16}\langle z_1\dot{z}_2 - z_2\dot{z}_1\rangle_{\mathcal{T}}, \quad \text{(A3)} \end{aligned}$$

that is Eq. (10).

Appendix B: Swimmer efficiency in the strong noise regime

The mean circulation frequency can be obtained from Eq. (51):

$$\langle\dot{\phi}\rangle = (1-\beta)\langle\sin\phi\cos\phi\rangle - \alpha\langle(\cos\phi)^2\rangle. \quad \text{(B1)}$$

The angular distribution $\rho(\phi)$ to be used in Eq. (B1), is obtained from the deformation PDF $\rho(\mathbf{z})$: $\rho(\phi) = \int_0^\infty z\mathrm{d}z\ \rho(\mathbf{z})$; $\rho(\mathbf{z}) = A\exp(-(1/2)Z^{-1}_{ij}z_iz_j)$, $Z_{ij} = \langle z_iz_j\rangle$. Using Eq. (52), we obtain, after little algebra:

$$\begin{aligned} \rho(\phi) &= B[C(\cos\phi)^2 \\ &+ D(\sin\phi)^2 + E\sin\phi\cos\phi]^{-1}, \quad \text{(B2)} \end{aligned}$$

where

$$\begin{aligned} &C = 1 + \beta + \alpha^2; \quad D = (1+\beta)\beta; \\ &E = 2\alpha\beta; \quad \text{(B3)} \end{aligned}$$

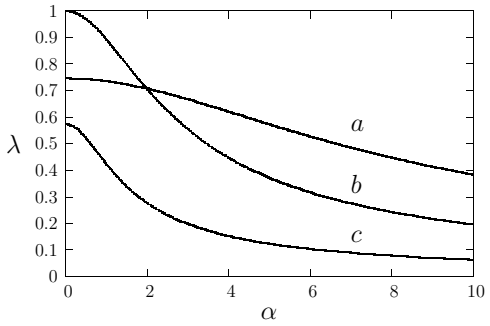


FIG. 4: Plot of the ratio $\lambda = \eta/\bar{\eta}$ vs α for three different values of β: (a) $\beta = 5.0$; (b) $\beta = 1.0$; (c) $\beta = 0.1$.

and B is a normalization. Adopting as definition of the stroke time: $\omega\mathcal{T} = 2\pi/\langle\dot{\phi}\rangle$, Eqs. (19), (53) and (54), give us, for the efficiency in the strong noise regime:

$$\lambda = \eta/\bar{\eta} = 2\langle\dot{\phi}\rangle/\alpha. \quad \text{(B4)}$$

Evaluation of the average in Eq. (B1), with the distribution in Eqs. (B2) and (B3), gives the result in Fig. 4. Equation (51) leads to an efficiency that is always below that of the corresponding optimal deterministic swimmer. Maximum efficiency is achieved for $\beta = 1$ and α small, which is, in some sense, a maximally isotropic forcing in deformation space. This is not a casual result. It is possible to see that a trimer obeying a symmetrized version of Eq. (51): $\dot{z}_1 + z_1 - \alpha z_1 = \xi_1$, $\dot{z}_2 + z_1 + \alpha z_2 = \xi_2$, is characterized by efficiency $\eta = \bar{\eta}$ for all values of α.

Acknowledgments

I wish to thank Paolo Muratore Ginanneschi and Carlos Mejia Monasterio for interesting and helpful conversation. This research was carried on in part at the Mathematics Department of the University of Helsinki, with financial support by the Center of Excellence "Analysis and Dynamics" of the Academy of Finland.

[1] S. Childress, *Mechanics of Swimming and Flying* (Cambridge University Press, Cambridge, U.K., 1981)

[2] E.M. Purcell, "Life at low Reynolds numbers", Am. J. Phys. **45**, 3 (1977)

[3] A. Shapere and F. Wilczek, "Geometry of self-propulsion at low Reynolds numbers", J. Fluid Mech. **198**, 557 (1989)

[4] R. Dreyfus, J. Baudry, M.L. Roper, M. Fermigier, H.A. Stone and J. Bibette, "Microscopic artificial swimmers" *Nature* **437**, 862 (2005)

[5] T.S. Yu, E. Lauga and A.E. Hosoi, *Phys. Fluids* **18**, 091701 (2006)

[6] B. Behkam and M. Sitti, *J. Dyn. Sys., Meas., Control* **128**, 36 (2006)

[7] M. Leoni, J. Kotar, B. Bassetti, P. Cicuta, M.C. Lagomarsino, *Soft Matter* **5**, 472 (2009)

[8] J. Lighthill, *Mathematical Biofluiddynamics* (SIAM, Philadelphia 1975)

[9] J.R. Blake, "Microbiological fluid mechanics: a tribute to Sir James Lighthill", Mathematical Methods in the Applied Sciences **24**, 1469 (2001)

[10] H.A. Stone and A.D.T. Samuel, "Propulsion of microorganisms by surface distorsions", Phys. Rev. Lett. **77**, 4102 (1996)

[11] L.E. Becker, S.A. Koehler and H.A. Stone "On self-propulsion of micro-machines at low Reynolds number: Purcell's three-link swimmer" J. Fluid Mech. **490**, 15 (2003)

[12] A. Najafi and R. Golestanian "Simple swimmer at low Reynolds number: Three linked spheres", Phys. Rev. E **69**, 062901 (2004)

[13] J.E. Avron, O. Gat and O. Kenneth "Optimal swimming at low Reynolds numbers", Phys. Rev. Lett. **93**, 186001 (2004)

[14] F. Schweitzer, W. Ebeling and B. Tilch, "Complex Motion of Brownian Particles with Energy Depots", Phys. Rev. Lett. **80**, 5044 (1998)

[15] T. Vicsek, *Fluctuations and scaling in biology*, (Oxford University Press, Oxford, 2001)

[16] V. Lobaskin, D. Lobaskin and I. Kulic, "Brownian dynamics of a microswimmer", Eur. J. Phys. Spec. Topics **157**, 149 (2008)

[17] R. Golestanian and A. Ajdari, "Stochastic low Reynolds number swimmers" J. Phys. Condens. Matter **21**, 204104 (2009)

[18] J. Dunkel and I.M. Zaid, "Noisy swimming at low Reynolds numbers", Phys. Rev. E **80**, 021903 (2009)

[19] R. Golestanian, T.B. Liverpool and A. Ajdari, "Propulsion of a molecular machine driven by asymmetric distribution of reaction products", Phys. Rev. Lett. **94**, 220801 (2005)

[20] W.E. Paxton, S. Sundararajan, T.E. Mallouk and A. Sen, "A. Catalytic Nanomotors: RemoteControlled Autonomous Movement of Striped Metallic Nanorods", Angew. Chem. Int. Ed. **45**, 5420 (2006)

[21] C.M. Pooley and A.C. Balazs, "Producing swimmers by coupling reaction-diffusion equations to a chemically responsive material", Phys. Rev. E **76**, 016308 (2007)

[22] R. Ma, G.S. Klindt, I.H. Riedel-Kruse, F. Jülicher and B. Friedrich, "Active phase and amplitude fluctuation of flagellar beating", (2014) ArXiv:1401.7036

[23] A.B. Kolomeisky and M.E. Fisher, "Molecular motors: a theoretist's perspective", Ann. Rev. Phys. Chem. **58**, 675 (2007)

[24] D.J. Earl, C.M. Pooley, J.F. Ryder, I. Bredberg and J.M. Yeomans, "Modeling microscopic swimmers at low Reynolds numbers", J. Chem. Phys. **126**, 064703 (2008)

[25] P. Olla, "Passive swimming in low Reynolds number flows", Phys. Rev. E, **82**, 015302(R) (2010)

[26] B.M. Friedrich and F. Yülicher "Flagellar Synchronization Independent of Hydrodynamic Interactions" Phys. Rev. Lett. **109**, 138102 (2012)

[27] G. P. Alexander, C. M. Pooley, and J. M. Yeomans, "Scattering of low-Reynolds-number swimmers", Phys. Rev. E **78**, 045302(R) (2008)

[28] V.B. Putz and J.M. Yeomans "Hydrodynamics Synchronization of Model Microswimmers", J. Stat. Phys. **137**, 1001 (2009)

[29] T.J. Murphy and J.L. Aguirre, "Brownian motion of N interacting particle. I. Extension of the Einstein diffusion relation to the N particle case", J. Chem. Phys. **57**, 2098 (1972)

[30] R. Golestanian and A. Ajdari, "Analytic results for the three-sphere swimmer at low Reynolds number", Phys. Rev. E **77**, 036308 (2008).

[31] P. Olla "Effective swimming strategies in low Reynolds number flows", Eur. Phys. J. B, **80**, 263 (2011)

[32] J. Happel and H. Brenner, *Low Reynolds Number Hydrodynamics*, (Kluwer, Boston, 1973)

[33] J.M.R. Parrondo, "Reversible ratchets as Brownian particles in an adiabatically changing periodi potential", Phys. Rev. E **57**, 7297 (1998)

[34] A. Shapere and F. Wilczek, "Self-propulsion at low Reynolds numbers", Phys. Rev. Lett. **58**, 2051 (1987)

[35] D.A. Sivak and G.E. Crooks, "Thermodynamics metrics and optimal paths", Phys. Rev. Lett. **108**, 190602 (2012)

[36] T. Schmiedl and U. Seifert, "Optimal finite-time processes in stochastic thermodynamics", Phys. Rev. Lett. **98**, 108301 (2007)

[37] E. Aurell, C. Mejia-Monasterio and P. Muratore-Ginanneschi "Boundary layers in stochastic thermodynamics", Phys. Rev. E **85**, 020103(R) (2012)

[38] E. Aurell, K. Gawedzki, C. Mejia-Monasterio, R. Mohayaee and P. Muratore-Ginanneschi, "Refined second law of thermodynamics for fast random processes", J. Stat. Phys. **147**, 487 (2012)

[39] E. Aurell, C. Mejia-Monasterio and P. Muratore-Ginanneschi, "Optimal protocols and optimal transport in stochastic thermodynamics", Phys. Rev. Lett. **106**, 250601 (2011)

[40] K. Sekimoto, "Langevin equations and thermodynamics", Prog. Theor. Phys. Supp. **130**, 17 (1998)

[41] Z. Schuss, *Theory and Application of Stochastic Differential Equations* (Wiley & Sons, New York, 1981)

[42] It is possible to see, from Eq. (2), that the kinetic energy of the trimer is diagonal in the center of mass velocity $\dot{x}_1^{\rm CM}$ and the deformation rates $\dot{z}_{1,2}$: $E = (3/2)m(\dot{x}_1^{\rm CM})^2 + (3/8)mR^2(\dot{z}_1^2 + \dot{z}_2^2)$ (to lowest order in a/R, we disregard the contribution from $\tilde{\mathbf{u}}_i$ to the bead velocities). The standard argument that each degree of freedom contributes $k_BT/2$ to the energy fluctuations then applies, and leads to Eqs. (20) and (21).